Distinct Properties of Titanate Nanosheets with Different Hydrodynamic Radii: A UV-Vis Spectroscopy and Titration Study

Tosapol Maluangnont[*1,2]

[1]*Electroceramic Research Laboratory, College of Nanotechnology, King Mongkut's Institute of Technology Ladkrabang, Bangkok, Thailand 10520*
[2]*Catalytic Chemistry Research Unit, Faculty of Science, King Mongkut's Institute of Technology Ladkrabang, Bangkok, Thailand 10520*

Abstract

The quantum size effect in two-dimensional (2D) materials is largely governed by their thickness in the nm-range but is less dependent on the lateral sizes. Here, "lateral sizes" are represented by the hydrodynamic radii (R_H) obtained from dynamic light scattering (DLS) which is a fast and efficient method of determining the particle size from the bulk. In this work, nanosheets with different R_H have been prepared by the exfoliation of a lepidocrocite titanate $H_{0.7}Ti_{1.825}O_4 \cdot H_2O$. The reagents employed include tetramethylammonium hydroxide (TMAOH) or tetrabutylammonium hydroxide (TBAOH). The R_H obtained is ~485 nm for nanosheets exfoliated with TMA^+, and 151 nm with TBA^+. The electronic structure of nanosheets was investigated by UV-vis spectroscopy. The λ_{max} at 266 nm for the colloidal suspension of large nanosheets shifts to 263 nm for the small ones. Tauc plots indicate the optical band gap of 3.68 eV for large nanosheets, and 3.82 eV for small nanosheets. The suspension of small nanosheets also shows a more pronounced bluish tint. The change to chemical properties of these nanosheets has also been investigated by titration experiments with diluted HCl. Starting from basic pH and extending to acidic one, an abrupt increase in R_H of large-size nanosheets occurs at a later stage (i.e., pH ~ 3.3), compared to the small-size nanosheets (pH ~ 4.2). At acidic pH, both types of nanosheets macroscopically reassembled into three-dimensional (3D) agglomerates visible by bare eyes. These agglomerates inherit the distinct chemical behaviour from their respective colloidal suspension, exhibiting different compactness. The controlled exfoliation of layered metal oxides to nanosheets of different hydrodynamic radii could be a simple way of tuning the chemical/physical properties of nanosheets and their higher-order assembly.

Keywords: Lepidocrocite titanate, Exfoliation, Nanosheets, tetraalkylammonium cations

1. Introduction

Two-dimensional (2D) nanomaterials have received great attention lately due to their potential applications in a variety of fields including photocatalysis [1], electrochemical energy storage [2], and electronics [3]. These materials are characterized by a high structural anisotropy and a large aspect ratio (lateral over thickness). The thickness of 2D materials (i.e., nanosheets) is in a nm-range, while the width and length can be up to a few millimeters. Such characters result in the quantum size effect, where charge carriers are allowed to move freely on the *xy* plane but not along the *z*-axis [4],[5]. This quantum confinement endows 2D materials unique physical/chemical properties unlike their 0D or 1D counterparts.

Corresponding Author E-mail: tosapol.ma@kmitl.ac.th

Titanate nanosheets are one of the first semiconducting nanosheets reported in the field with a wide range of applications [6-8]. A unilamellar nanosheet is 0.75 nm-thick, comprising of four atomic planes. The nanosheets were made via a soft chemistry approach starting from microcrystals of lepidocrocite titanate such as $Cs_{0.7}Ti_{1.825}O_4$ [6]. This structure consists of the negatively-charged edge-shared TiO_6 octahedra extending on the *ac* plane of the orthorhombic unit cell [9-14]. The sheets stack on top of each other along the *b*-direction with Cs^+ located at the interlayer spaces. Typically, the proton exchange first occurs in such a fashion that the crystals are converted into the protonated form with expanded interlayer distance. After that, the material is treated with tetraalkylammonium hydroxide (TAAOH, $(C_nH_{2n+1})_4NOH$). This large cation serves as an exfoliating agent, causing the infinite separation of lepidocrocite sheets into a colloidal suspension of unilamellar nanosheets.

It has been shown recently that the lateral sizes of nanosheets prepared by this approach can be controlled [15]. Here, "lateral sizes" are represented by the hydrodynamic radii (R_H) obtained from dynamic light scattering (DLS) which is a fast and efficient method of determining the particle size from the bulk. For example, relatively small nanosheets (R_H ~200 nm) were obtained from $K_{0.88}Li_{0.27}Ti_{1.73}O_4$ when using tetrabutylammonium cations (TBA^+, $(C_4H_9)_4N^+$) as the exfoliating agent. On the other hand, the use of tetramethylammonium cations (TMA^+, $(CH_3)_4N^+$) gives relatively large nanosheets with R_H up to 8 μm. These nanosheets possess different swelling behaviour, including some optical properties [15]. However, the quantum size effect in these nanosheets has not been demonstrated despite a 40-fold difference in R_H. The results from this method contrasts with the sonication-assisted exfoliation of transition metal dichalcogenides such as WS_2. In this case, not only a shift in the optical extinction spectra but also differences in electrocatalytic activities were observed, depending on the length of the nanosheets [16].

In this article, the exfoliation of $H_{0.7}Ti_{1.825}O_4 \cdot H_2O$ into nanosheets with different "particle sizes" was accomplished by the treatment with TMAOH or TBAOH. The two suspensions of nanosheets show a 3-fold difference in R_H. Yet, a small shift in the UV-vis absorption spectra was detected, suggesting the dependence of the electronic structure on the lateral sizes. The distinct chemical behavior of these two nanosheets was further investigated by (i) titration experiments, and (ii) by observation of the macroscopically reassembled materials.

2. Experimental

Solid state synthesis and chemical exfoliation.

Lepidocrocite titanate $Cs_{0.7}Ti_{1.825}O_4$ was synthesized from the reported method by calcining the mixture of Cs_2CO_3 and TiO_2 (1 to 5.3 in mole ratio) at 1073 K for 20 h. The titanate was subjected to three cycles of proton exchange using 1 M HCl (1 g of solid to 100 mL of the solution) with the acid renewed every cycle [6],[15]. Then, the solid was washed with deionized water until it is free from acid, followed by drying at room temperature. The composition $H_{0.7}Ti_{1.825}O_4 \cdot H_2O$ was assumed for the protonated lepidocrocite titanate following the previous work [6]. Exfoliation of the titanate was achieved by the mechanical shaking of the mixture containing 0.4 g of $H_{0.7}Ti_{1.825}O_4 \cdot H_2O$ with 100 mL of TMAOH (or TBAOH) at 180 rpm for 14 days. The mole ratio of proton in the solid to the tetraalkylammonium cation is fixed at 1/1. The colloidal dispersion prepared with TMAOH (TBAOH) will be hereafter called "nanosheets(M)" (or "nanosheets(B)"). TMAOH (10% in water) and TBAOH (40% in water) are the products of Acros Organics. Others chemicals

Corresponding Author E-mail: tosapol.ma@kmitl.ac.th

are of reagent grade and were used as received, except Cs_2CO_3 which was dried at 120 ºC overnight prior to use.

Characterization.

Powder X-ray diffraction (PXRD) measurements were conducted on a Rigaku DMAX 2200/Ultima+ diffractometer, employing a Cu-Kα radiation at 40 kV and 30 mA. The sample was scanned in the range 2θ = 5-65º at a 0.05 degree/step and a detection time of 0.6 second/step. FTIR spectra were directly measured on the powder (without mixing with KBr) by a Perkin Elmer spectrometer (Spectrum Two) at the resolution of 4 cm^{-1}. For TGA (Perkin-Elmer, Pyris 1), the sample was heated from room temperature to 900 ºC (10 ºC/min) under nitrogen gas flowing at 20 mL/min.

For UV-vis measurements, an amount of 0.2 mL of the original suspension was diluted to a total volume of 100 mL. The spectra were recorded from this diluted suspension using a T90+ UV/VIS spectrometer (PG Instruments) from 200 to 800 nm. Deionized water was used for baseline subtraction. Dynamic light scattering (DLS) was performed on the original suspension (i.e., without dilution) using a Delsa™ Nano Particle Size Analyzer (Beckman Coulter). The hydrodynamic radii (R_H) of the nanosheets were calculated using Stokes-Einstein equation, assuming that nanosheets are rigid spheres [17]. For each suspension, ten measurements giving the symmetric profile of the size distribution was recorded. AFM images of the nanosheets deposited on a Si substrate were taken with an SPA-400 system (SPA400, Seiko Instruments Inc.) in noncontact mode using a Si probe. The nanosheet suspension was diluted to a concentration of 0.08 g/L before the pH was adjusted to 9. The nanosheets were deposited onto a polyethylenimine (PEI)-coated substrate as described previously [15].

Titration experiments and electrostatic assembling.

The pH of the (undiluted) suspension prior to and after the titration with a small portion of ~0.02 M HCl was measured by a Starter 2100 pH meter (Ohaus). Then, the resulting colloid was withdrawn and placed into a cuvette for DLS measurements. In the electrostatic assembling, 10 mL of the suspension was mixed with 10 mL of ~0.02 M HCl. The whole content was transferred into a cylinder. The apparent volume fraction of agglomerates relative to the total volume (20 mL) was then compared.

3. Results and Discussion

Synthesis of protonated lepidrocrocite titanate

The white powder obtained after calcining the mixture of Cs_2CO_3 and TiO_2 at 1073 K for 20 h was subject to three cycles of proton exchange with 1 M HCl. The PXRD pattern of the solid shown in Fig. 1a is the characteristics of the lepidocrocite titanate structure. The pattern can be indexed based on an orthorhombic unit cell with a = 0.3790(3), b = 1.843(3) and c = 0.2953(5) nm [18-19]. The unit cell parameters obtained in this work are in reasonable agreement with values reported by Sasaki et al of a = 0.3783(2), b = 1.8735(8) and c = 0.2978(2) nm [19]. In this structure, the negatively-charged sheets of edge-shared TiO_6 octahedra extend on the *ac* plane. The sheets stack on top of each other along the *b*-direction with the repeating interlayer distance of $b/2$ = 0.9215 nm with H_3O^+ in between.

The successful synthesis of the protonated lepidocrocite titanate is also supported by the FTIR spectrum of the product shown in Fig. 1b. The peaks at 642 and 915 cm^{-1} representthe Ti-O vibration of the TiO_6 octahedra [11],[19-20]. The band at 3226 and 1655 cm^{-1} can be ascribed to the stretching and bending vibration of H_2O adsorbed on the external surfaces respectively [11],[19-20]. The presence of these two bands agrees well with the presence of water molecules, where the interlayer Cs^+ is exchanged with H_3O^+. As shown in Fig. 1c, this product losses its weight by 10% (RT to 120 ^oC) and 5% (120-650 ^oC), in good agreement with the previous work [19]. So, one can infer that the protonated lepidocrocite titanate $H_{0.7}Ti_{1.825}O_4 \cdot H_2O$ can be successfully synthesized.

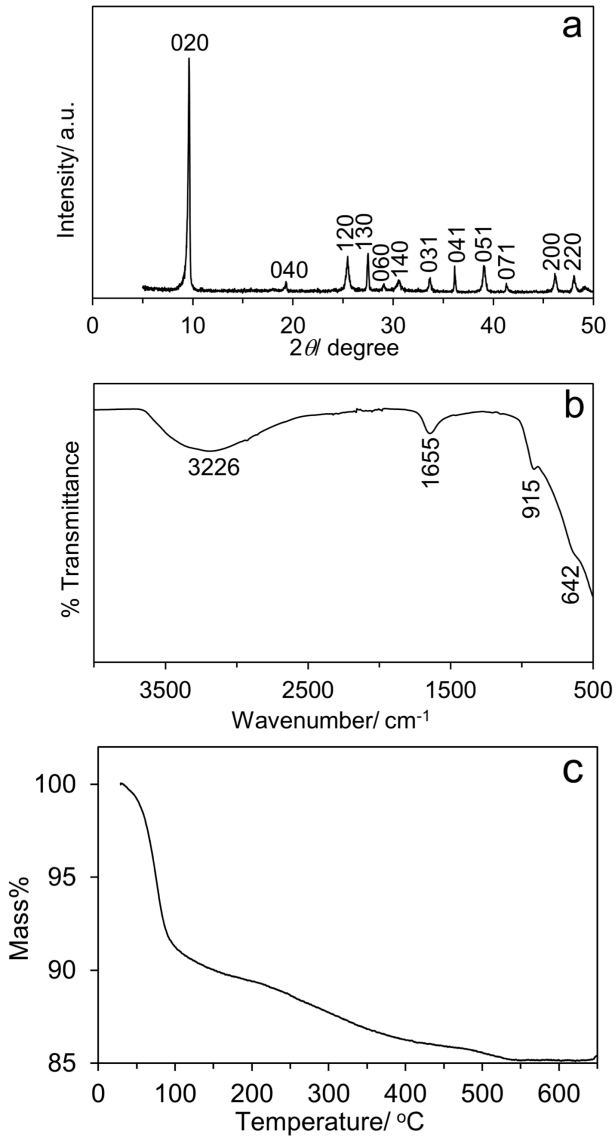

Fig. 1. (a) PXRD pattern, (b) FTIR spectrum, and (c) mass loss curve of the protonated lepidocrocite titanate $H_{0.7}Ti_{1.825}O_4 \cdot H_2O$.

Exfoliation to nanosheets

The powder of protonated lepidocrocite titanate was mechanically shaken with TMAOH (or TBAOH) for 14 days. The mixture initially containing the suspended powder and the clear solution gradually transformed into colloidal suspension. This observation indicates the infinite separation of stacks of layers in protonated lepidocrocite titanate into individual layers known as nanosheets [6], [15]. As shown in the inset of Fig. 2, the white suspension prepared with TBA^+ (i.e., nanosheets(B)) has a more pronounced bluish tint than the suspension prepared with TMA^+ (nanosheets(M)). A small difference in the appearance of these two suspensions suggests that the absorption/transmission/scattering of light by nanosheets are not equal. As suggested previously, the less-pronounced bluish tint in nanosheets(M) may be a result of the intense light scattering associated with large size dispersed objects [15].

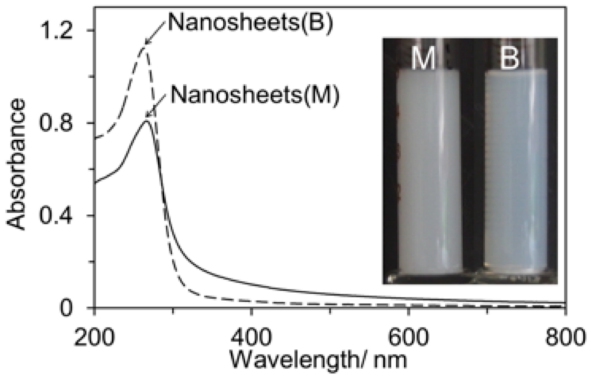

Fig. 2. UV-vis spectra of the colloidal suspensions of nanosheets prepared from the exfoliation of $H_{0.7}Ti_{1.825}O_4 \cdot H_2O$ with TMA^+ (nanosheets(M)) or with TBA^+ (nanosheets(B)). The inset is the photograph showing the appearance of the suspension. A more pronounced bluish tint of nanosheets(B) can be observed.

The overall shape of the UV-vis absorption spectra of these two suspensions shown in Fig. 2 is similar to the reported characteristics of lepidocrocite titanate (exfoliated with TBA^+) with a peak at ~265 nm [6]. However, when compared to the literature, three distinct features of these two suspensions must be noted [6]. Firstly, there is a shift in the wavelength of the maximum absorbance (λ_{max}) from 266 nm for nanosheets(M) to 263 nm for nanosheets(B). This small but noticeable change in λ_{max} suggests the change in the electronic structure of these two suspensions, likely due to the effect of the lateral-size. Secondly, nanosheets(M) exhibit a substantial absorption from 300 to 600 nm well above the baseline level. In fact, Tauc plots were derived from the UV-vis spectra and are shown in Fig. 3. The direct band gap E_g of 3.82 eV for nanosheets(B) is in excellent agreement with the literature [5]. Meanwhile, the nanosheets(M) show the E_g of 3.68 eV.

Finally, using the experimentally determined absorbance A and the molar extinction coefficient $\varepsilon = 1.2\times10^4$ mol^{-1} dm^3 cm^{-1} at 265 nm, the concentration 6.48×10^{-5} mol L^{-1} was obtained for nanosheets(M), and 9.18×10^{-5} mol L^{-1} for nanosheets(B) [21]. The 1.5-fold smaller concentration of nanosheets(M) might be explained by the slow exfoliation kinetics of TMA^+ relative to TBA^+ as deduced previously from statistical AFM analysis [15].

Corresponding Author E-mail: tosapol.ma@kmitl.ac.th

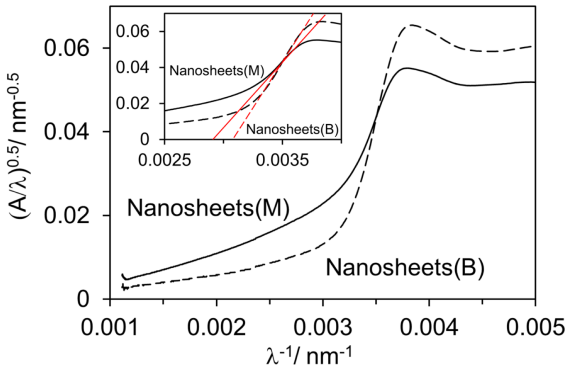

Fig. 3. Tauc plots derived from the UV-vis spectra of the colloidal suspensions of nanosheets from the exfoliation of $H_{0.7}Ti_{1.825}O_4 \cdot H_2O$ with TMA^+ (nanosheets(M)) or with TBA^+ (nanosheets(B)). The inset is the zoom-in showing the extrapolation to the intercept at the *x*-axis.

Dynamic light scattering (DLS) was employed to analyse the "particle size" (more correctly, the hydrodynamic radius R_H) of the nanosheets. The R_H of 485 nm was obtained from nanosheets(M), and 152 nm from nanosheets(B), i.e., a difference by a factor of 3. Typically, DLS assumes that particles of interest are spherical and rigid [17]. Both of these assumptions are not valid for two-dimensional (2D) objects like nanosheets because they are highly anisotropic and also flexible. Yet, DLS provides a fast and convenient estimation of "particle size" in the suspension [15], [17]. The relatively large "particle size" of nanosheets(M) in comparison to nanosheets(B) has been previously explained considering the mechanical stress experienced by the microcrystals upon the introduction of tetraalkylammonium cations [15]. While TMA^+ can penetrate deep into the crystals, the relatively large TBA^+ induces the cleavage and fragmentation of the crystals in the early stages of the intercalation.

A representative AFM image of the nanosheets(M) in Fig. 4 clearly shows several 2D objects. An example of the height profile (i.e., the thickness in the rage 1.1-1.4 nm) of three sheets is also shown. Although the crystallographic thickness along the b direction of the 2D lepidocrocite layer is ~0.75 nm, the slightly larger thickness found here (and also by others [15]) is probably because of the adsorption of water molecules and/or TMA^+ on its surface [7]. The distribution of lateral sizes in Fig. 4 is rather common, and might reflect the heterogeneity in the fragmentation of lepidocrocite titanate microcrystals [15]. As discussed previously (e.g., in layered zeolite MCM-22P), it is difficult to directly compare the lateral size from AFM with RH from DLS, as these two quantities characterize the nanosheets in different physical states [22].

Titration measurements and electrostatic reassembling

The two nanosheets have a subtle difference in chemical reactivities as shown by the pH-dependence change in the RH upon titration with diluted HCl. Results are shown in Fig. 5. Considering the suspension of nanosheets(B) as an example. At the starting pH of 9.1, RH is 161 nm. The RH remains relatively constant at 160(17) nm until the pH is down to 7.8. Upon further addition of HCl, RH gradually increases as the pH decreases: 233(9) nm (7.4 > pH > 6.6), 395(86) nm (5.9> pH > 5.4), 791 nm (pH = 4.7) and ~1,800 nm (pH = 4.2). At the pH value of 3.9, a large RH of 8 μm at the upper limit of the instrument was obtained.

The change in the ionic strength (upon addition of HCl) results in the change in the thickness of a diffuse double layer around the negatively-charged nanosheets [23], [24]. There is an increase in electrostatics interactions such that the nanosheets reassembled macroscopically into three-dimensional (3D) network.

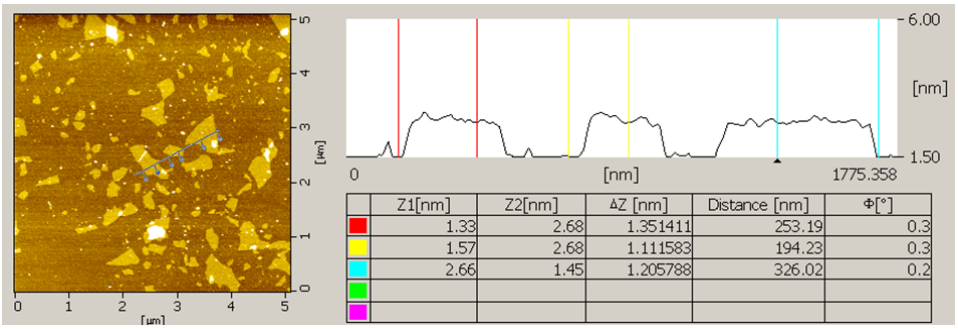

Fig. 4. A representative AFM image (covering the area of 5×5 μm^2) of nanosheets(M) obtained from the exfoliation of $H_{0.7}Ti_{1.825}O_4 \cdot H_2O$ with TMA^+. The thickness of three nanosheets is also shown.

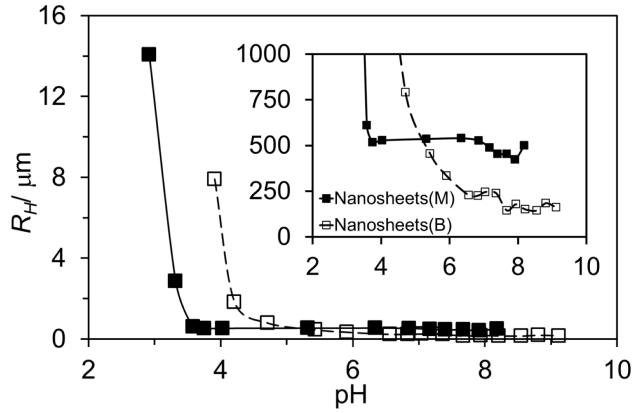

Fig. 5. The change in the hydrodynamic radius (R_H) of the nanosheets obtained from the exfoliation of $H_{0.7}Ti_{1.825}O_4 \cdot H_2O$ with TMA^+ (nanosheets(M)) or TBA^+ (nanosheets(B)). The inset is the zoom-in showing the abrupt change in R_H.

The pH dependence of R_H in the suspension of nanosheets(M) shows similar behaviour, although with differences in the exact values (Fig. 5). The R_H right after the exfoliation (pH 8.2) is 500 nm. In the range 7.9 > pH > 3.6, R_H remains relatively unchanged at 508(54) nm. Lowering the pH to 3.3 and 2.9 results in the R_H of ~2,800 nm and 14 μm, respectively. The value of 14 μm is above the upper limitation and should be considered with care. The inset of Fig. 5 focuses around the pH range where there is an abrupt change in R_H. One can see that such a rise is quite early (i.e., pH ~ 4.2) for nanosheets(B) with relatively small "particle size". The sharp increase in the "particle size" does not occur for nanosheets(M) until the pH value of ~ 3.3 is reached. Our results suggest that protonation could first occur at the edges (which are more abundant on relatively small nanosheets(B)). The difference in the onset pH showing a sharp increase in R_H translates to a difference in the proton concentration of $10^{(4.2-3.3)}$ = 7.9 M, for nanosheets differing in the "particle size" by a factor of 1.5.

Corresponding Author E-mail: tosapol.ma@kmitl.ac.th

These nanosheets with different values of R_H, when reassembled by the addition of protons, give the macroscopic sample with different texture. The photos in Fig. 6 are obtained from the experiment where 10 mL of ~0.02 M HCl was mixed with 10 mL of the suspension. The fluffy agglomerates were generated and settled to the bottom of the container, in good qualitative agreement with the increase in R_H observed in the titration measurement. The apparent volume fraction of the agglomerates relative to the total volume of the mixture is 0.45 for nanosheets(M), and 0.35 for nanosheets(B). This result suggests that the reassembled nanosheets(B) is rather compact while the reassembled nanosheets(M) could have considerable porosities. Such distinct physical properties might be explained by the differences in the orientations of reassembled nanosheets, the inclusion of water molecules, the formation of interconnected pores, etc., which are dependent on R_H.

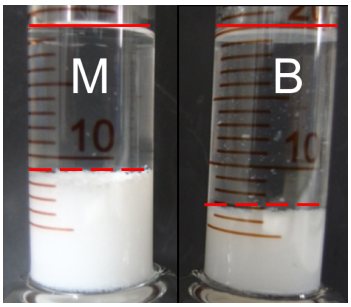

Fig. 6. Photographs showing the agglomerates obtained when 10 mL of ~0.02 M HCl was mixed with 10 mL of nanosheets(M) (left) or nanosheets(B) (right). The full line and dash line at the top and middle of the photos mark the top surfaces of the water and the agglomerates, respectively.

4. Conclusion

In this article, the quantum size effect in two-dimensional (2D) materials differing in their hydrodynamic radii is reported. Lepidocrocite titanate nanosheets have been prepared by exfoliating the protonated $H_{0.7}Ti_{1.825}O_4 \cdot H_2O$ with either TMA^+ or TBA^+. The R_H of 485 nm was obtained by DLS measurement from nanosheets(M), and 151 nm from nanosheets(B), i.e., a difference by a factor of 3. UV-vis spectroscopy indicates that the colloidal suspension of large-size nanosheets prepared with TMA^+ shows λ_{max} = 266 nm and E_g = 3.68 eV. On the other hand, λ_{max} = 263 nm and E_g = 3.82 eV were obtained from small-size nanosheets exfoliated with TBA^+. The R_H gradually increased when pH of the suspensions decreased upon titration with HCl, resulting in the formation of a 3D macroscopic assembly. The exfoliation of layered metal oxides to nanosheets of variable "lateral sizes" could be a simple way of tuning the chemical/physical properties of nanosheets and their higher-order assembly.

References

[1] D. Deng, X.K.S. Novoselov, Q. Fu, N. Zheng, Z. Tian and X. Bao, Nature *Nanotechnology* 11 (2016), 218.

[2] M. Shao, R. Zhang, Z. Li, M. Wei, D. G. Evans and X. Duan, *Chemical Communication* 51 (2015), 15880.

[3] G. Fiori, F. Bonaccorso, G. Iannaccone, T. Palacios, D. Neumaier, A. Seabaugh, S. K. Banerjee, L. Colombo, *Nature Nanotechnology* 9 (2014), 768.

[4] K. Nakamura, Y. Oaki and H. Imai, *Journal of American Chemical Society* 135 (2013), 4501.
[5] N. Sakai, Y. Ebina, K. Takada and T. Sasaki, *Journal of American Chemical Society* 126 (2004), 5851.
[6] T. Sasaki and M. Watanabe, *Journal of American Chemical Society* 120 (1998), 4682.
[7] T. Sasaki and M. Watanabe, *Journal of Physical Chemistry B* 101 (1997), 10159.
[8] L. Wang and T. Sasaki, *Chemical Reviews* 114 (2014), 9455.
[9] D. Groult, C. Mercey and B. Raveau, *Journal of Solid State Chemistry* 32 (1980), 289.
[10] A.F. Reid, W.G. Mumme and A.D. Wadsley, *Acta Crystallographica* B24 (1968), 1228.
[11] T. Sasaki, F. Kooli, M. Iida, Y. Michiue, S. Takenouchi, Y. Yajima, F. Izumi, B.C. Chakoumakos and M. Watanabe, *Chemistry of Materials* 10 (1998), 4123.
[12] T. Gao, P. Norby, H. Okamoto and H. Fjellvåg, *Inorganic Chemistry* 48 (2009), 9409.
[13] T. Gao, H. Fjellvåg and P. Norby, *Journal of Material Chemistry* 19 (2009), 787.
[14] T. Gao, H. Fjellvåg and P. Norby, *Chemistry of Materials* 21 (2009), 3503.
[15] T. Maluangnont, K. Matsuba, F. Geng, R. Ma, Y. Yamauchi and T. Sasaki, *Chemistry of Materials* 25 (2013), 3137.
[16] Z. Gholamvand, D. McAteer, A. Harvey, C. Backes and J.N. Coleman, *Chemistry of Materials* 28 (2016), 2641.
[17] Y. Yue, Y. Kan, H. Choi, A. Clearfield and H. Liang, *Applied Physics Letters* 107 2015, 253103.
[18] I.E. Grey, C. Li, I.C. Madsen and J.A. Watts, *Journal of Solid State Chemistry* 66 (1987), 7.
[19] T. Sasaki, M. Watanabe, Y. Michiue, Y. Komatsu, F. Izumi and S. Takenouchi, *Chemistry of Materials* 7 (1995), 1001.
[20] T. Maluangnont, P. Arsa, K. Limsakul, S. Juntarachairot, S. Sangsan, K. Gotoh, and T. Sooknoi, *Journal of Solid State Chemistry* 238 (2016), 175.
[21] T. Sasaki, Y. Ebina, K. Fukuda, T. Tanaka, M. Harada and M. Watanabe, *Chemistry of Materials* 14 (2002), 3524.
[22] T. Maluangnont, Y. Yamauchi, T. Sasaki, W.J. Roth, J. Čejka and M. Kubu, *Chemical Communications* 50 (2014), 7378.
[23] R. Besselink, T.M. Stawski, H.L. Castricum, D.H.A. Blank, J.E. ten Elshof, *Journal of Physical Chemistry C* 114 (2010), 21281.
[24] H. Yuan, D. Dubbink, R. Besselink and J. E. ten Elshof, *Angewandte Chemie International Edition* 54 (2015), 9239.

Corresponding Author E-mail: tosapol.ma@kmitl.ac.th